THE INFLUENCE OF ELEMENT INTERACTION AND MATERIAL NONLINEARITY ON THE ULTIMATE CAPACITY OF STAINESS STEEL CROSS-SECTIONS

Marios Theofanous
Lecturer (ΠΔ 407/80)
Department of Civil Engineering, Aristotle University of Thessaloniki
Thessaloniki, Greece
e-mail: mariosgt@civil.auth.gr

Leroy Gardner
Reader
Department of Civil Engineering and Environmental Engineering, Imperial College London
London, UK
e-mail: leroy.gardner@imperial.ac.uk

ABSTRACT

The effect of element interaction and material nonlinearity on the ultimate capacity of stainless steel plated cross-sections is investigated in this paper. The focus of the research lies in cross-sections failing by local buckling; member instabilities, distortional buckling and interactions thereof with local buckling are not considered. The cross-sections investigated include rectangular hollow sections (RHS), I sections and parallel flange channels (PFC). Based on previous finite element investigations of structural stainless steel stub columns, parametric studies were conducted and the ultimate capacity of the aforementioned cross-sections with a range of element slendernesses and aspect ratios has been obtained. Various design methods, including the effective width approach, the direct strength method (DSM) and the continuous strength method (CSM) were assessed on the basis of the numerical results. Element interaction has been shown to be significant for slender cross-sections, whilst the behaviour of stocky cross-sections is more strongly influenced by the material strain-hardening characteristics. A modification to the continuous strength method has been proposed to allow for the effect of element interaction, which leads to more reliable ultimate capacity predictions.

1. INTRODUCTION

The treatment of local buckling within the framework of EN 1993-1-4 [1], the European structural design rules for stainless steel, draws heavily from the respective design guidance for carbon steel EN 1993-1-1 [2] and follows the familiar cross-section classification approach. The constituent plate elements of a cross-section are placed into discrete behavioural classes by comparing their width to thickness ratio with codified slenderness limits, which depend on the element's boundary conditions, the applied stress gradient and the manufacturing process (whether cold-formed or welded). The cross-section itself is classified according to its most slender constituent element. Since the constituent plate elements are treated in isolation, the effect of element interaction on both the elastic buckling and ultimate response is neglected. Boundary conditions at element junctions are assumed to be simply-supported (i.e. zero rotational stiffness), as reflected in the plate buckling coefficients k_σ specified in EN 1993-1-5 [3]. However, the embedded conservatism is not uniform for all cross-sections, but varies, depending on how close the actual boundary conditions are to the assumed ones.

Ignoring element interaction is a simplifying assumption common to both carbon steel and stainless steel. A further simplifying assumption which has greater significance for stainless steel is that of a bilinear (elastic, perfectly-plastic) material response, which ensures consistency between carbon steel and stainless steel design specifications. The deviation of stainless steel's stress-strain response from that of carbon steel is depicted in Fig. 1. Despite the absence of a well-defined yield point, an equivalent yield stress, termed the 0.2% proof stress $\sigma_{0.2}$, is employed and an elastic, perfectly-plastic material response is assumed for stainless steel as for carbon steel, thereby neglecting the actual material behaviour and pronounced strain-hardening. This assumption is of little significance for very slender elements, the failure of which is governed by stiffness, but severely compromises accuracy and design efficiency in the case of stocky stainless steel plated elements, failure of which is mainly governed by material response.

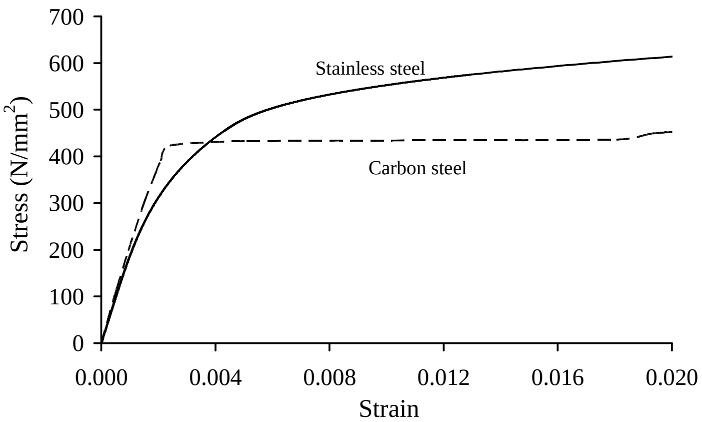

Fig. 1: Indicative stainless steel and carbon steel stress-strain behaviour

With the increasing usage of high strength stainless steel grades, which effectively leads to more slender cross-sections, together with the high initial material cost associated with stainless steel, reassessing the validity of the aforementioned assumptions and eliminating any associated conservatism is warranted. Advanced design methods that allow for element interaction, actual material response or both, which have been previously employed or proposed for carbon steel and/or stainless steel components, are discussed hereafter.

2. DESIGN METHODS FOR THE TREATMENT OF LOCAL BUCKLING

The method of cross-section classification coupled with the effective width approach, which was originally derived for carbon steel [4, 5] and later adapted to stainless steel [6] is employed in most stainless steel design specifications for the treatment of local buckling. The width of any constituent plate element that is classified as Class 4 (slender) is reduced to an effective width (which is a function of the element slenderness) to account for loss of effectiveness due to local buckling. Although conceptually simple, application of the effective width method is often cumbersome, since having established the effective width of the individual elements, calculation of the properties of the effective cross-section is then required. Moreover, it may have to be applied iteratively, when a shift of a cross-section's neutral axis and a corresponding modification of the applied stress distribution is caused by the loss of effectiveness of some parts of the cross-section.

The cumbersome nature of the effective width method when applied to slender cold-formed steel cross-sections of complex geometries and concerns about its ability to account for all possible failure modes including interaction buckling, led to the development of the Direct Strength Method (DSM) by Schafer and Peköz [7], a review of which is given by Schafer [8]. The DSM is based on determining the strength of a structural component as an explicit function of its gross cross-sectional properties, elastic critical buckling stresses for all relevant instability modes (i.e. global buckling, local buckling and distortional buckling) and yield strength. To this end, a linear eigenvalue buckling analysis of the full cross-section by means of the constrained finite strip method is utilised [9] and the relevant critical stresses are obtained. In the present paper the software CUFSM [9] has been utilised. The DSM has been calibrated on the basis of numerous test data on cold-formed carbon steel components and has been adopted in the North American [10] and Australian [11] specifications for cold-formed steel design as an alternative design method to the effective width approach. It should be noted that the DSM assumes a bilinear elastic-perfectly plastic material response and is therefore best suited to the treatment of slender cross-sections and components, the failure of which is mainly governed by elastic buckling and post-buckling and remains largely unaffected by strain-hardening.

To account for the pronounced effect of strain-hardening on the capacity of stainless steel cross-sections, the Continuous Strength Method (CSM) was proposed for the treatment of local buckling of stainless steel cross-sections [12, 13]. The basis of the method lies in an experimentally derived 'base' curve, calibrated against all available stub column test data, which relates a cross-section's slenderness, denoted $\bar{\lambda}_p$, to its deformation capacity, denoted ε_{LB}. The cross-section slenderness $\bar{\lambda}_p$ is assumed to equal the slenderness of the most slender constituent plate element, determined according to EN 1993-1-4 [1]. The deformation capacity ε_{LB} is the maximum attainable strain for a given cross-section in compression or the outer fibre strain of an assumed linear strain distribution of a cross-section in bending. The deformation capacity is utilized in conjunction with an accurate material law, which in the case of stainless steel is a compound Ramberg-Osgood model [14], to obtain the corresponding stress σ_{LB}. Additional features of the method include an explicit equation to account for corner strength enhancements [15]. The method explicitly accounts for strain-hardening and does not impose unnecessary limitations on the maximum attainable stress. However, it does not account for the effect of element interaction on the local buckling capacity of the cross-section.

3. NUMERICAL MODELLING

The accuracy of the previously described design methods is assessed hereafter on the basis of an extensive numerical study conducted on stainless steel stub columns by means of the general purpose finite element (FE) programme ABAQUS [16]. The FE models were developed following the guidelines given in [17, 18], which were shown to give accurate capacity predictions. The cross-sections considered herein include RHS (with SHS as a special case), PFC and I sections with the focus being on local buckling alone. All cross-sections had an outer flange width of 100 mm, whilst the web height and cross-section thickness were varied to obtain a wide range of local slendernesses and aspect ratios. For all RHS and PFC sections the internal root radii were assumed to be equal to the cross-section thickness. A uniform section thickness was assumed for RHS and PFC, whereas two flange-to-web thickness ratios were considered for the I sections. Each stub column length was fixed to three times the largest cross-section dimension. A total of 65 geometric configurations were considered, a summary of which is given in Table 1.

Cross section	Outer flange width (mm)	Ratio of web to flange outer dimensions (aspect ratio)	Flange thickness (mm)	Web to flange thickness ratio	No. of geometric configurations considered
RHS	100	1, 2, 3	8, 6, 5, 4, 3	1	15
I sections	100	1, 1.5, 2	8, 6, 5, 4, 3	1, 0.6	30
PFC	100	1, 2, 3, 4	8, 6, 5, 4, 3	1	20

Table 1: Geometric configurations modelled in the parametric studies

The models were discretized with the reduced integration 4-noded doubly curved general-purpose shell element S4R with finite membrane strains. All degrees of freedom were fixed at the stub columns' ends except for the vertical displacement at the loaded edge. Kinematic coupling was employed to impose uniform end-shortening at the loaded edge. A linear eigenvalue buckling analysis was initially conducted to extract the lowest buckling mode shape for each cross-section; this was thereafter introduced as the geometric imperfection pattern in the subsequently performed geometrically and materially non-linear analyses. Typical lowest elastic buckling mode shapes and failure modes for the different cross-section types are depicted in Fig. 2. The amplitude of the geometric imperfection was given by a modification to the Dawson and Walker [19] model, proposed in [17]. The compound Ramberg-Osgood model initiated by Mirambell and Real [14], as modified in [12] was incorporated in the FE models in the true stress–logarithmic plastic strain format. Two sets of material properties were considered in the parametric studies for each modelled cross-section, resembling a typical austenitic stainless steel and a typical duplex stainless steel. The adopted material properties were taken form an extensive statistical analysis on mill certificate data carried out by Groth and Johansson [20] and are given in Table 2. A detailed account of the numerical studies is given in [21].

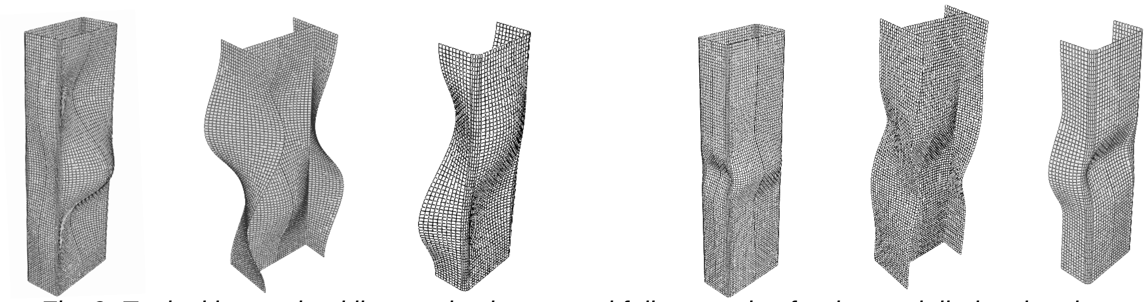

Fig. 2: Typical lowest buckling mode shapes and failure modes for the modelled stub columns

Material	E (N/mm^2)	$\sigma_{0.2}$ (N/mm^2)	$\sigma_{1.0}/\sigma_{0.2}$	n	$n_{0.2,1.0}$
Austenitic	200000	306.1	1.20	5.6	2.7
Duplex	200000	592.0	1.15	5.0	3.4

Table 2: Material properties employed in the parametric studies

4. RESULTS AND DISCUSSION

An overview of the accuracy attained by each method is given in Table 3, where the mean value and coefficient of variation of the predicted capacities normalized by the FE ultimate load are given for each type of cross-section and each design method considered in the present study. As expected, the design methods not allowing for stresses greater than the $\sigma_{0.2}$ result in excessively conservative design resistances for stocky cross-sections and a corresponding dependence of the predictions on the cross-sectional slenderness, as depicted in Figs. 3 and 4. Moreover it can be observed that the DSM displays superior consistency in the low to medium slenderness range compared to the CSM.

Cross-section	EN 1993-1-4		DSM		CSM		Modified CSM	
	MEAN	COV	MEAN	COV	MEAN	COV	Mean	COV
RHS	0.86	0.09	0.84	0.09	1.00	0.08	0.96	0.08
I sections	0.86	0.07	0.84	0.07	0.94	0.11	0.97	0.08
PFC	0.86	0.08	0.88	0.08	1.02	0.11	0.99	0.04
All	0.86	0.08	0.85	0.08	0.98	0.11	0.97	0.07

Table 3: Comparison between design method predictions of compression resistance and FE results

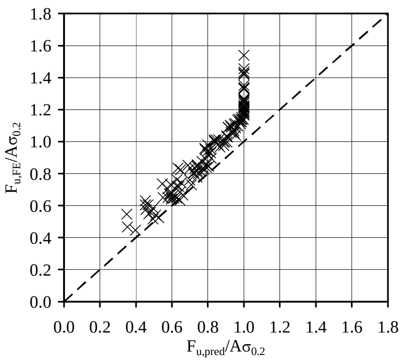

Fig. 3: Comparison between FE and predicted compression resistances for the DSM

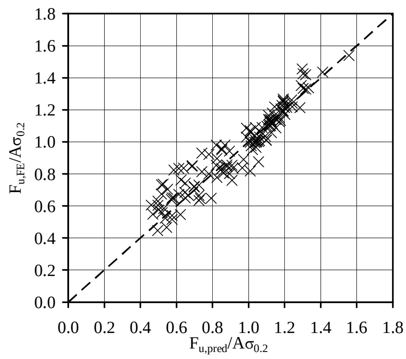

Fig. 4: Comparison between FE and predicted compression resistances for the CSM

The definition of the cross-sectional slenderness $\bar{\lambda}_l$ utilized in the DSM is adopted herein as a modification to the CSM; hence the critical buckling stress of the whole cross-section, derived by means of CUFSM [9], is incorporated into the definition of cross-section slenderness. The cross-section slenderness is thereafter utilized to obtain the normalized deformation capacity $\varepsilon_{LB}/\varepsilon_0$, and finally the stress at failure σ_{LB} via the compound Ramberg-Osgood constitutive law. The modified CSM equation Eq. (1), as derived on the basis of the FE results, reads:

$$\frac{\varepsilon_{LB}}{\varepsilon_0} = \frac{1.22}{\bar{\lambda}_l^{\,2.71-0.69\bar{\lambda}_l}} \le 15 \quad \text{for } \bar{\lambda}_l \le 1.8 \qquad (1)$$

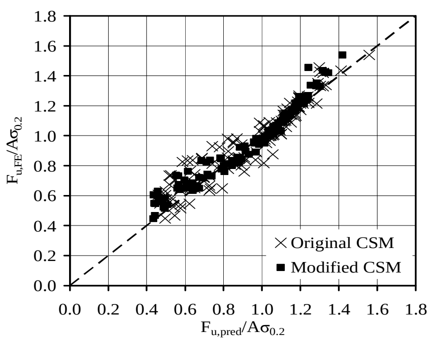

Fig. 5: Comparison between FE and predicted compression resistances

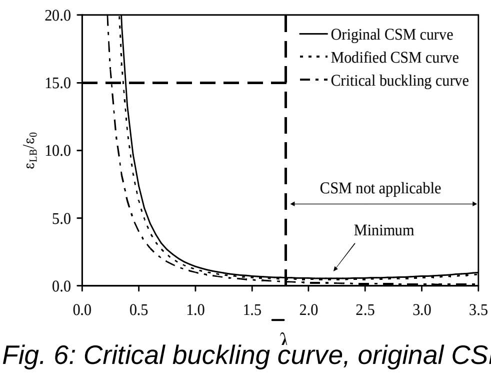

Fig. 6: Critical buckling curve, original CSM design curve and modified CSM design curve

The predictions of the modified CSM are displayed together with those of the original CSM in Fig. 5 and Table 3, where a significant reduction in scatter is observed. An upper slenderness limit of $\bar{\lambda}_l$=1.8 and an upper limit of $\varepsilon_{LB}/\varepsilon_0$=15 on the exploitation of strain-hardening, is proposed herein. The new CSM curve is plotted together with the original CSM curve and the elastic critical buckling curve in Fig. 6.

5. CONCLUSIONS

Various design methods for the treatment of local buckling in stainless steel cross-sections have been outlined in the present paper and their relative merits and drawbacks have been highlighted. The cross-section classification coupled with effective width approach treats plate elements individually and assumes a bilinear elastic perfectly-plastic material constitutive law. More advanced methods include the direct strength method (DSM) and the continuous strength method (CSM). Based on an extensive parametric study on stainless steel stub columns, all methods have been assessed and the value of incorporating both element interaction and material nonlinearity within one design method was highlighted. A modification to the CSM, by redefining the considered slenderness to include element interaction, has been described. The modified CSM combines the merits of both the original CSM and the DSM and has been shown to offer accurate capacity predictions.

6. REFERENCES

[1] EN 1993-1-4. (2006) Eurocode 3: Design of steel structures - Part 1.4: General rules - Supplementary rules for stainless steel. CEN.

[2] EN 1993-1-1 (2005) Eurocode 3. Design of Steel Structures: Part 1-1: General rules and rules for buildings. CEN.

[3] EN 1993-1-5 (2006) Eurocode 3. Design of Steel Structures: Part 1-5: Plated structural elements. CEN.

[4] Winter, G. "Strength of thin steel compression flanges", Bulletin No. 35/3, Engrg. Experiment Sta., Cornell University, Ithaca, N.Y, 1947.

[5] Winter, G. "Performance of thin steel compression flanges", Bulletin No. 33, Engrg. Experiment Sta., Cornell University, Ithaca, N.Y, 1950.

[6] Johnson, A.L. and Winter, G. "Behaviour of stainless steel columns and beams", Journal of the Structural Division, ASCE, Vol. 92, No. ST5, 1966, pp. 97-118.

[7] Schafer, B., Peköz, T. "Direct strength prediction of cold-formed steel members using numerical elastic buckling solutions", Thin-walled structures, research and developments. NewYork: Elsevier, 1998, pp. 127-144.

[8] Schafer, B.W. "Review: The Direct Strength Method of cold-formed steel member design", Journal of Constructional Steel Research, Vol. 64, No. 7-8, 2008, pp. 766-778.

[9] Schafer, B.W., Ádány, S. “Buckling analysis of cold-formed steel members using CUFSM: conventional and constrained finite strip methods.” Eighteenth International Specialty Conference on Cold-Formed Steel Structures, Orlando, FL. October 2006.

[10] North American Specification. “Appendix 1: Design of cold-formed steel structural members using the Direct Strength Method”, In: 2004 supplement to the North American Specification for the design of cold-formed steel structures. Washington (DC): American Iron and Steel Institute: 2004.

[11] Standards Australia. “Cold-formed steel structures AS/NZS 4600: 2005”, Sydney, Australia, 2005.

[12] Gardner, L. and Nethercot, D.A. “Experiments on stainless steel hollow sections - Part 1: Material and cross-sectional behaviour”, Journal of Constructional Steel Research, Vol. 60, No. 9, 2004, pp. 1291-1318.

[13] Ashraf, M., Gardner, L. and Nethercot, D.A. “Compression strength of stainless steel cross-sections”, Journal of Constructional Steel Research, Vol. 62, No. 1-2, 2006, pp. 105-115.

[14] Mirambell, E. and Real, E. “On the calculation of deflections in structural stainless steel beams: an experimental and numerical investigation”, Journal of Constructional Steel Research, Vol. 54, No. 1, 2000, pp. 109-133.

[15] Cruise, R.B. and Gardner, L. “Strength enhancements induced during cold forming of stainless steel sections”, Journal of Constructional Steel Research, Vol. 64, No. 11, 2008, pp. 1310-1316.

[16] ABAQUS. ABAQUS/Standard user’s manual volumes I-III and ABAQUS CAE manual. Version 6.6. (Pawtucket, USA): Hibbitt, Karlsson & Sorensen, Inc, 2006.

[17] Gardner, L. and Nethercot D.A. “Numerical Modeling of Stainless Steel Structural Components-A Consistent Approach”, Journal of Structural Engineering, ASCE, Vol. 130, No. 10, 2004, pp. 1586-1601.

[18] Theofanous, M. and Gardner, L. “Testing and numerical modelling of lean duplex stainless steel hollow section columns”, Engineering Structures, Vol. 31, No. 12, 2009, pp. 3047-3058.

[19] Dawson, R.G. and Walker, A.C. “Post-buckling of geometrically imperfect plates”, Journal of the Structural Division, ASCE. Vol. 98, No. ST1, 1972, pp. 75-94.

[20] Groth, H.L. and Johansson, R.E. “Statistics of the mechanical strength of stainless steels”, Proceeding of the Nordic Symposium on Mechanical Properties of Stainless Steels SIMR, Sigtuna, Sweden, 1990, pp. 17-31.

[21] Theofanous, M. “Studies of the nonlinear response of stainless steel structures”, PhD Thesis, Structures Section, Department of Civil and Environmental Engineering, Imperial College, London, 2010.

Η ΕΠΙΡΡΟΗ ΤΗΣ ΑΛΛΗΛΕΠΙΔΡΑΣΗΣ ΤΩΝ ΠΛΑΚΟΛΩΡΙΔΩΝ ΚΑΙ ΤΗΣ ΚΡΑΤΥΝΣΗΣ ΣΤΗ ΦΕΡΟΥΣΑ ΙΚΑΝΟΤΗΤΑ ΔΙΑΤΟΜΩΝ ΑΝΟΞΕΙΔΩΤΟΥ ΧΑΛΥΒΑ

Μάριος Θεοφάνους
Λέκοτρας (ΠΔ 407/80)
Τμήμα πολιτικών μηχανικών Α.Π.Θ.
Θεσσαλονίκη, Ελλάδα
e-mail: mariosgt@civil.auth.gr

Leroy Gardner
Reader
Department of Civil Engineering and Environmental Engineering, Imperial College London
London, UK
e-mail: leroy.gardner@imperial.ac.uk

ΠΕΡΙΛΗΨΗ

Η παρούσα εργασία πραγματεύεται την επιρροή της αλληλεπίδρασης των πλακολωρίδων που συναποτελούν μια διατομή και της κράτυνσης του υλικού στη φέρουσα ικανότητα διατομών ανοξείδωτου χάλυβα. Η εργασία επικεντρώνεται σε διατομές που αστοχούν σε τοπικό λυγισμό, ενώ άλλες μορφές λυγισμού καθώς και αλληλεπιδράσεις αυτών με τον τοπικό λυγισμό δεν μελετώνται. Οι μελετηθείσες διατομές περιλαμβάνουν ορθογωνικές κοιλοδοκούς (RHS), διατομές U και διατομές διπλού ταυ. Βάσει των αποτελεσμάτων μιας εκτεταμένης παραμετρικής μελέτης με πεπερασμένα στοιχεία, αξιολογούνται διάφορες μέθοδοι αντιμετώπισης του τοπικού λυγισμού, συμπεριλαμβανομένης της μεθόδου του ενεργού πλάτους που υιοθετείται από τον Ευρωκώδικα EN 1993-1-4, της μεθόδου άμεσης αντοχής (Direct Strength Method) και της μεθόδου συνεχούς αντοχής (Continuous Strength Method). Η παραμετρική μελέτη αναδεικνύει τη σημασία της αλληλεπίδρασης των πλακολωρίδων στον τοπικό λυγισμό διατομών μεγάλης λυγηρότητας καθώς και την επιρροή της κράτυνσης στη φέρουσα ικανότητα διατομών μικρής λυγηρότητας. Στα πλαίσια της εργασίας προτείνεται μία τροποποίηση της μεθόδου συνεχούς αντοχής, μέσω της οποίας λαμβάνεται υπόψη η αλληλεπίδραση των πλακολωρίδων και η οποία οδηγεί σε ακριβέστερες προβλέψεις της φέρουσας ικανότητας διατομών ανοξείδωτου χάλυβα.